Front. Phys. 11(5), 110503 (2016)
DOI 10.1007/s11467-016-0575-4

RESEARCH ARTICLE

Design of diamond-shaped transient thermal cloaks with homogeneous isotropic materials

Ting-Hua Li (李廷华)[1,2], **Dong-Lai Zhu** (朱东来)[1], **Fu-Chun Mao** (毛福春)[2], **Ming Huang** (黄铭)[2,†], **Jing-Jing Yang** (杨晶晶)[2], **Shou-Bo Li** (李寿波)[1]

[1] *Technical Center of China Tobacco Yunnan Industrial Co., Ltd., Kunming 650231, China*
[2] *School of Information Science and Engineering, Yunnan University, Kunming 650091, China*
Corresponding author. E-mail: †huangming@ynu.edu.cn

Received November 21, 2015; accepted February 3, 2016

Transformation thermodynamics as a major extension of transformation optics has recently received considerable attention. In this paper, we present two-dimensional (2D) and three-dimensional (3D) diamond-shaped transient thermal cloaks with non-singular homogeneous material parameters. The absence of singularity in the parameters results from the fact that the linear coordinate transformation is performed by expanding a line segment rather than a point into a region, while the mechanism behind the homogeneity is the homogeneous stretching and compression along orthogonal directions during the transformation. Although the derived parameters remain anisotropic, we further show that this can be circumvented by considering a layered structure composed of only four types of isotropic materials based on the effective medium theory. Numerical simulation results confirm the good performance of the proposed cloaks.

Keywords transformation thermodynamics, metamaterials, thermal cloak, effective medium theory

PACS numbers 05.70.-a, 44.10.+i, 81.05.Zx

Frontiers of Physics

1 Introduction

The field of transformation optics [1, 2] has recently attracted significant attention because it provides a general method for designing novel functional devices that possess the ability to control the behavior of electromagnetic waves in a desired way. A wide variety of devices with unusual properties have been proposed and fuelled by the rapid development of metamaterials [3–10], including invisible cloaks, concentrators, and illusion devices. Inspired by these pioneering works, the field of transformation optics has been gradually extending from electromagnetic waves to acoustic waves [11], elastic waves [12], matter waves [13], and surface plasmon waves [14]. Moreover, the underlying idea extends beyond the scope of the systems exhibiting waves, and is also valid for the problems of mass diffusion [15] and thermal conduction [16]. The fundamental reason for such an extension is that the governing equations describing these systems are form-invariant under coordinate transformations.

Based on the form-invariance of the thermal conduction equation, transformation thermodynamics as an emerging field has opened up a new avenue for arbitrary manipulations of thermal current by using metamaterials. It has also helped to define a revolutionary design paradigm that enables researchers to build astonishing thermal devices that were previously deemed impossible or unconceivable, such as thermal cloaks, concentrators, and rotators [17–36]. Among these various applications, conventional thermal cloaks, capable of guiding a thermal flux around an enclosed region, have been by far the most interesting. Potential application of these cloaks for thermal protection bears significance in almost every area, ranging from engineering to modern military applications. Circular and ellipsoidal conventional thermal cloaks were first proposed by Fan *et al.* [17], following which square-shaped and arbitrarily shaped cloaks were also reported [18–20]. Because the coordinate transformation is performed by expanding a point into a region along the radial direction, the material parameters of the proposed cloaks are not only singular but also anisotropic and inhomogeneous. To overcome these difficulties, some more feasible strategies were presented for designing thermal cloaks with finite constant conductivity [21–23]. The foregoing investigations are very attractive, but their common characteristic is that all aforementioned cloaks only operate in the steady state. For most practical applications, a device that can operate in a transient state is more favorable or even necessary. Recently, a transient thermal cloak was suggested for controlling the dynamic thermal current, but it is worth noting that this cloak must be implemented by using $2N$ types of different isotropic materials, where N is the total number of discretization layers [24]. From a practical point of view, the requirement for such a large number of materials may give rise to complicated fabrication problems that may impede the successful implementation of a thermal cloak. More recently, transient thermal cloaks comprising only two or five isotropic materials were proposed [25–29]. However, to the best of our knowledge, transient thermal cloaks with non-circular/non-spherical shapes have been barely studied.

In this paper, inspired by the work of Li *et al.* [5], we propose two-dimensional (2D) and three-dimensional (3D) diamond-shaped transient thermal cloaks, based on transformation thermodynamics. The advantage of these thermal cloaks is that the linear coordinate transformation is conducted by expanding a line segment instead of a point into a region along the orthogonal direction, making the cloak material parameters non-singular and homogeneous. To further remove the anisotropy in the material parameters, we present a 2D layered thermal cloak as an example for discussing the isotropic realization method. Distinct from the previously proposed transient thermal cloak [24], the isotropic materials required for such a layered cloak are independent of the number of discretization layers, and the cloak can be implemented by using only four types of isotropic materials. The thermal cloaking effect of the designed cloaks was validated by performing numerical simulations. This work suggests a different method of designing transient thermal cloaks with simple material parameters, and is of potentially high guiding significance for practical fabrication of diamond-shaped thermal cloaks.

2 Method and simulation model

The basic principle of transformation thermodynamics is the form-invariance of the thermal conduction equation under the coordinate transformation. For a transient state and without a heat source, the general thermal conduction equation in the original space is given by

$$\rho C\frac{\partial T}{\partial t} = \nabla\cdot(\kappa\nabla T)\,, \tag{1}$$

where ρ, C, and κ are the density, the specific heat capacity and the thermal conductivity of the background material, respectively. $\partial T/\partial t$ is the derivative of temperature T with respect to time t and ∇ is the gradient operator. Note that for the special case of a steady state, the time-dependent term vanishes; thus, in this case ρ and C play no role and only κ is relevant. Guenneau *et al.* [24] have proposed that the thermal conduction equation should retain its form under the coordinate transformation; thus, Eq. (1) in the transformed space can be written as:

$$\rho' C'\frac{\partial T}{\partial t} = \nabla'\cdot(\kappa'\nabla' T)\,. \tag{2}$$

Note that Eqs. (1) and (2) have the same structure, except that the material parameters (i.e., ρ', C', and κ') in the transformed space take the following form:

$$\kappa' = \begin{pmatrix} \kappa'_{xx} & \kappa'_{xy} & \kappa'_{xz} \\ \kappa'_{yx} & \kappa'_{yy} & \kappa'_{yz} \\ \kappa'_{zx} & \kappa'_{zy} & \kappa'_{zz} \end{pmatrix} = \frac{J\kappa J^T}{\det(J)},$$

$$\rho' C' = \frac{\rho C}{\det(J)}, \tag{3}$$

where $J = \frac{\partial(u,v,w)}{\partial(x,y,z)} = \begin{pmatrix} \partial u/\partial x & \partial u/\partial y & \partial u/\partial z \\ \partial v/\partial x & \partial v/\partial y & \partial v/\partial z \\ \partial w/\partial x & \partial w/\partial y & \partial w/\partial z \end{pmatrix}$ is the Jacobian transformation matrix from the original space (x, y, z) to the transformed space (u, v, w). J^T and $\det(J)$ are the transpose and the determinant of the Jacobian matrix J, respectively.

Figure 1 shows the schematic of the coordinate transformation for the design of the proposed 2D diamond-shaped transient thermal cloak. The transformation proceeds in two steps, which is analogous to that used in Ref. [5] for the 2D electromagnetic invisible cloak. The line segment $2a$ in the original space [see Fig. 1(a)] is first stretched to $2b$ in the transitional space [see Fig. 1(b)], and then the stretched line segment $2b$ is further expanded into a diamond-shaped cloaking region *be-b-e* in the transformed space [see Fig. 1(c)]. It should be mentioned that the smaller is the value of a (resulting in the line segment $2a$ closer to a point), the better is the cloaking effect. Following the two-step mapping

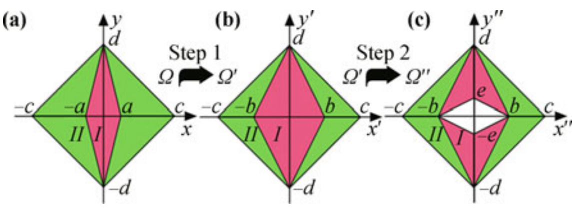

Fig. 1 Schematic of the coordinate transformation for the design of 2D diamond-shaped transient thermal cloak: **(a)** → **(b)** the line segment $2a$ is stretched to $2b$ in the x direction; **(b)** → **(c)** the line segment $2b$ is expanded into a diamond-shaped region *be-b-e*.

procedure outlined above, the transformation equations from the original space to the transformed space are

$$x'' = \frac{b}{a}x, \quad y'' = -\frac{e}{a}x\mathrm{sgn}(xy) + \frac{(d-e)}{d}y + e\mathrm{sgn}(y),$$
$$z'' = z \tag{4}$$

for region I (the red region) and

$$x'' = \frac{c-b}{c-a}x - \frac{c}{d}\frac{(a-b)}{(a-c)}y\mathrm{sgn}(xy) + \frac{c(a-b)}{a-c}\mathrm{sgn}(x),$$
$$y'' = y, \quad z'' = z \tag{5}$$

for region II (the green region). Note that in Eqs. (4) and (5) the functions sgn(xy), sgn(x), and sgn(y) are the sign functions and the values returned by them are determined by the signs of xy, x, and y, respectively. After substituting Eqs. (4) and (5) into Eq. (3), the material parameters of the 2D diamond-shaped transient thermal cloak are obtained as

$$\kappa'_I = \begin{pmatrix} \frac{bd}{a(d-e)} & -\frac{de}{a(d-e)}\mathrm{sgn}(xy) & 0 \\ -\frac{de}{a(d-e)}\mathrm{sgn}(xy) & \frac{d^2e^2 + a^2(d^2-e^2)}{abd(d-e)} & 0 \\ 0 & 0 & \frac{ad}{b(d-e)} \end{pmatrix}\kappa, \quad \rho'_I C'_I = \frac{ad}{b(d-e)}\rho C \tag{6}$$

in region I and

$$\kappa'_{II} = \begin{pmatrix} \frac{d^2(c-b)^2 + c^2(a-b)^2}{d^2(c-a)(c-b)} & \frac{c(b-a)}{d(b-c)}\mathrm{sgn}(xy) & 0 \\ \frac{c(b-a)}{d(b-c)}\mathrm{sgn}(xy) & \frac{c-a}{c-b} & 0 \\ 0 & 0 & \frac{c-a}{c-b} \end{pmatrix}\kappa, \quad p'_{II} C'_{II} = \frac{c-a}{c-b}\rho C \tag{7}$$

in region II. The geometrical parameters of the 2D thermal cloak in this article were set to $a = 0.02$ mm, $b = 0.2$ mm, $c = 0.4$ mm, $d = 0.4$ mm, and $e = 0.1$ mm. With these parameters, Eqs. (6) and (7) can be further expressed as:

$$\kappa'_I = \begin{pmatrix} 13.333 & -6.667\mathrm{sgn}(xy) & 0 \\ -6.667\mathrm{sgn}(xy) & 3.408 & 0 \\ 0 & 0 & 0.133 \end{pmatrix}\kappa,$$
$$p'_I C'_I = 0.133\rho C, \tag{8}$$
$$\kappa'_{II} = \begin{pmatrix} 0.953 & -0.9\mathrm{sgn}(xy) & 0 \\ -0.9\mathrm{sgn}(xy) & 1.9 & 0 \\ 0 & 0 & 1.9 \end{pmatrix}\kappa,$$
$$p'_{II} C'_{II} = 1.9\rho C. \tag{9}$$

The function sgn(xy) is equal to 1 in the first and third quadrants and −1 in the second and fourth quadrants; thus, the material parameters of the cloak are spatially invariant (i.e., homogeneous) once the geometrical parameters are fixed. In addition, the material parameters exhibit no singular values. As a result, it is possible to construct this 2D transient thermal cloak by using non-singular homogeneous materials. Compared with the previous work [29], in which the coordinate transformation started from a small circle rather than a point along the radial direction so that the singularity was avoided while the inhomogeneity still existed, the material parameters of the proposed cloak are not only non-singular but also homogeneous. The physical origin lies in the linear transformation, which expands a line segment instead of a point into a region along the orthogonal direction. It is undoubtedly true that a similar idea can be applied for designing a 3D transient thermal cloak, but the derivation of material parameters for this case is not included herein for brevity.

To some extent, non-singular homogeneous material parameters can reduce the fabrication difficulty of the cloak, but there is no denying that the parameters are still anisotropic. According to the effective medium theory, anisotropy can be eliminated by considering a layered structure composed of alternating layers of two different isotropic materials. To further facilitate the practical realization of the proposed device, we are now concerned with the question of how to build a transient thermal cloak by using isotropic materials.

For simplicity but without loss of generality, we consider here a 2D transient thermal cloak. Figure 2 shows the schematic of the layered structure for obtaining the proposed 2D thermal cloak. Regions I and II in the different quadrants are first divided into N layers, and then each anisotropic layer is mimicked by the double-layered

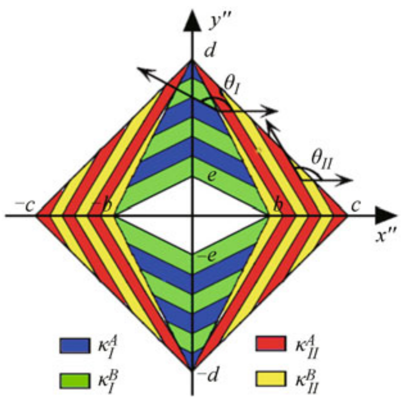

Fig. 2 Schematic of a layered structure for realizing a 2D diamond-shaped transient thermal cloak.

isotropic materials (layers A and B). Next, the derivation of isotropic material parameters for a 2D layered thermal cloak is described in detail. For the 2D case, only κ'_{xx}, κ'_{xy}, κ'_{yx}, κ'_{yy}, and $\rho' C'$ components of the material parameters are relevant. The symmetry of the thermal conductivity tensors in Eqs. (8) and (9) ensures that there always exists a rotation transformation that can map a symmetric tensor into a diagonal one:

$$\kappa''_i = \begin{pmatrix} \kappa_{i\hbar} & 0 \\ 0 & \kappa_{i\lambda} \end{pmatrix} \quad (i = I, II) \tag{10}$$

for regions I and II, in which the diagonal components $\kappa_{i\hbar}$ and $\kappa_{i\lambda}$ are determined by the following equations:

$$\kappa_{i\hbar} = \frac{\kappa'_{ixx} + \kappa'_{iyy} + \sqrt{\left(\kappa'_{ixx} - \kappa'_{iyy}\right)^2 + \left(2\kappa'_{ixy}\right)^2}}{2}, \tag{11a}$$

$$\kappa_{i\lambda} = \frac{\kappa'_{ixx} + \kappa'_{iyy} - \sqrt{\left(\kappa'_{ixx} - \kappa'_{iyy}\right)^2 + \left(2\kappa'_{ixy}\right)^2}}{2}. \tag{11b}$$

Furthermore, from the rotation transformation, the relation between the rotation angle θ_i and the thermal conductivity κ'_i can be written as

$$\tan(2\theta_i) = \frac{2\kappa'_{ixy}}{\kappa'_{ixx} - \kappa'_{iyy}}. \tag{12}$$

Assuming that the thicknesses of layers A and B are identical, the parameters of isotropic materials are given by

$$\kappa_i^A = \kappa_{i\hbar} + \sqrt{\left(\kappa_{i\hbar}\right)^2 - \kappa_{i\hbar}\kappa_{i\lambda}},$$
$$\kappa_i^B = \kappa_{i\hbar} - \sqrt{\left(\kappa_{i\hbar}\right)^2 - \kappa_{i\hbar}\kappa_{i\lambda}}, \quad \rho_i C_i = \rho'_i C'_i. \tag{13}$$

By combining Eqs. (8) and (9) with Eqs. (11)–(13), the isotropic material parameters and the rotation angles for regions I and II can be easily calculated and are given as follows: $\kappa_I^A = 33.333\kappa$, $\kappa_I^B = 0.03\kappa$, $\rho_I C_I = 0.133\rho C$, $\theta_I = 153.5°$, and $\kappa_{II}^A = 4.673\kappa$, $\kappa_{II}^B = 0.214\kappa$, $\rho_{II} C_{II} = 1.9\rho C$, $\theta_{II} = 121°$. It is not difficult to find that a 2D layered transient thermal cloak can be realized by using only four types of isotropic materials, regardless of the number of layers into which the regions are divided, just as shown in Fig. 2. This feature is quite different from what is exhibited by previously reported circular layered transient thermal cloaks [24], in which the isotropic materials required to build the cloak were always twice the number of discretization layers. Therefore, this work describes an alternative method for designing a transient thermal cloak with fewer types of isotropic materials, compared with the circular cloak. In the next section, we report the results of numerical simulations that were performed by using the commercial software COMSOL Multiphysics to demonstrate the performance of the proposed thermal cloaks.

3 Numerical simulations and discussion

For the sake of convenience of performing the simulations, the cloaking region and the background material were assumed to be stainless steel at room temperature, and the material density, specific heat capacity, and thermal conductivity were set to $\rho = 7850 \mathrm{kg/m^3}$, $C = 500 \mathrm{J/(kg \cdot K)}$ and $\kappa = 15 \mathrm{W/(m \cdot K)}$, respectively. As a matter of fact, the material of the cloaking region was arbitrarily alterable, and the cloak performed well even when the cloaking region and the background were filled with different materials; however, these considerations extend beyond the scope of this paper, because here, we mainly focused on validating the effectiveness of the proposed method.

First, numerical simulations were performed to validate the performance of the 2D ideal transient thermal cloak. Figures 3(a)–(c) show the temperature distribution for the proposed 2D diamond-shaped thermal cloak, captured at different times as the heat diffused along the x-axis. The left and right sides of the computational domain had constant temperature ($T = 600$ K and $T = 293.15$ K, respectively), and the top and bottom sides had insulation boundary conditions. The solid lines represent the isothermal lines and the arrows denote the thermal flux. The temperature distribution for the cloaking region without the cloak was also simulated for comparison, and the corresponding results are shown in Figs. 3(d)–(f). As can be seen from Figs. 3(a)–(c), the heat flows spontaneously from the left to the right owing to a thermal gradient between the two sides. The isothermal lines and thermal flux bend smoothly around the cloaking region, similar to water flowing around a pebble in

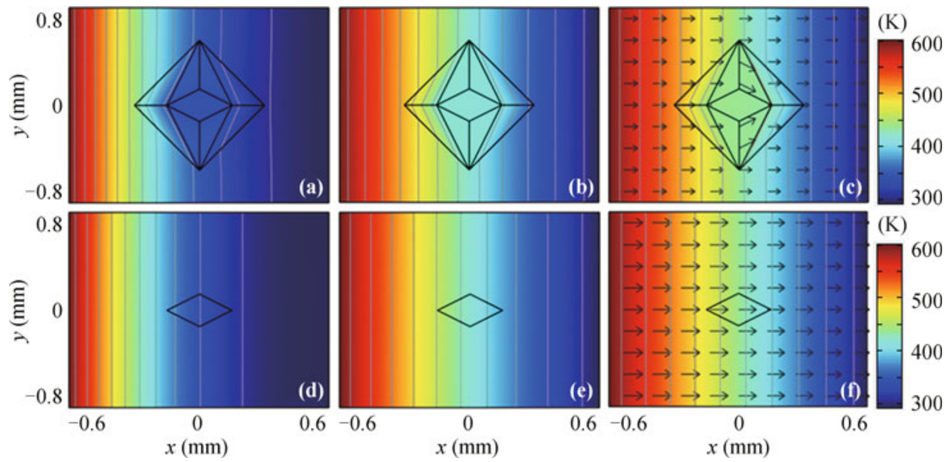

Fig. 3 Temperature distribution for a 2D diamond-shaped transient thermal cloak at different times **(a)** $t = 0.05$ s, **(b)** $t = 0.15$ s, **(c)** $t = 0.25$ s. **(d, e, f)** are the corresponding simulation results of (a)–(c) when the cloaking region is not surrounded by the proposed cloak. The solid lines represent the isothermal lines and the arrows denote the pathway of the thermal flux.

a stream. However, note that since the inner boundary *be-b-e* of the proposed cloak is not made of a perfect thermally insulating material with zero thermal conductivity, some thermal flux slightly diffuses into the cloaking region and the temperature monotonically increases with time until $t = 0.25$ s. For $t > 0.25$ s, the thermal system reaches the equilibrium state and the temperature inside the cloaking region becomes constant. Such a thermal cloak might find applications in protecting the sensitive regions of electrical circuits or chips from excessive heating. Moreover, a system of electronically connected components located inside the cloak would be able to perform optimally owing to the absence of thermal gradients between its components.

Because the thermal cloak is designed based on the transformation that comprises expanding a line segment instead of a point into a region, it is imperative to study the effect of the line segment length on the cloak performance, especially when a thermal gradient is normal to the equivalent line segment. Four cases, with line segment lengths of 0.04 mm, 0.16 mm, 0.28 mm, and 0.4 mm were considered. Figures 4(a)–(d) show the temperature distribution in the vicinity of a 2D diamond-shaped transient thermal cloak at $t = 0.25$ s for these four cases, in which the heat diffuses from the top to the bottom. It is evident that with increasing the length of the line segment, the cloaking effect of the cloak gradually worsens. In particular, when the line segment length is 0.28 mm or longer, the system almost does not function as a thermal cloak because the thermal flux cannot detour the cloaking region under these circumstances. Consequently, line segments shorter than 0.28 mm are acceptable for real applications.

Next, for more realistic applications, we considered a 3D diamond-shaped transient thermal cloak with non-

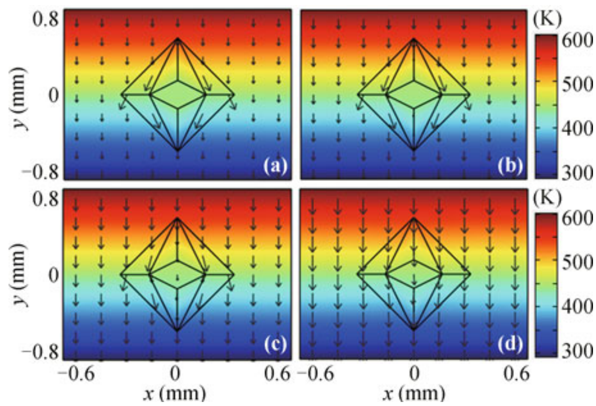

Fig. 4 Temperature distribution at $t = 0.25$ s for a 2D diamond-shaped transient thermal cloak with an equivalent line segment length $2a = 0.04$ mm **(a)**, 0.16 mm **(b)**, 0.28 mm **(c)**, and 0.4 mm **(d)**. The heat diffuses from the top to the bottom and the arrows denote the pathway of the thermal flux.

singular material parameters. The temperature was set to 600 K and 293.15 K at the top and bottom sides of the cuboid-shaped computational domain, and the other four sides had insulation boundary conditions. We note here that similar simulation results were obtained for cloaks of different sizes. The temporal evolution of the distribution of temperature for a micro-sized 3D thermal cloak is shown in Fig. 5. The arrows in Fig. 5(d) show the thermal flux. As time elapses, the heat exhibits a simple flow from the hot to the cold region, and the temperature inside the cloaking region increases steadily until it reaches a plateau for $t \geqslant 0.75$ s. Besides, as indicated by the arrows, the thermal fluxes are regularly guided around the cloaking region and eventually return to their original flow pattern. That is to say, the cloak affects the dynamic thermal diffusion in its surroundings to conceal itself and any objects inside it from an exterior detector. Therefore, these simulations validate the

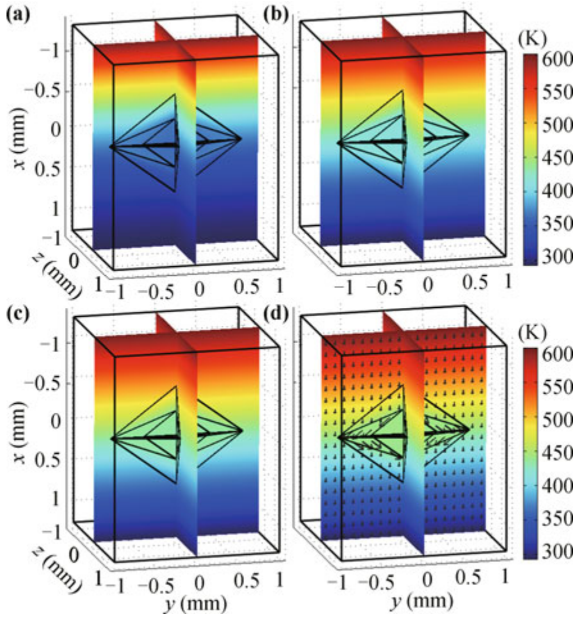

Fig. 5 Temperature distribution for a 3D diamond-shaped transient thermal cloak at different times **(a)** $t = 0.15$ s, **(b)** $t = 0.35$ s, **(c)** $t = 0.55$ s, and **(d)** $t = 0.75$ s. The arrows denote the pathway of the thermal flux.

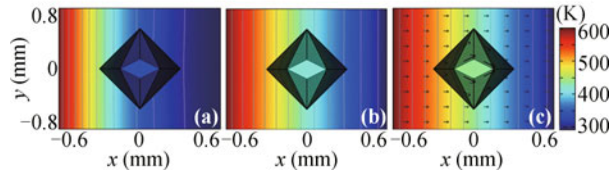

Fig. 6 Temperature distribution for a 2D layered transient thermal cloak at different times **(a)** $t = 0.05$ s, **(b)** $t = 0.15$ s, **(c)** $t = 0.25$ s. The solid lines represent the isothermal lines and the arrows denote the pathway of the thermal flux.

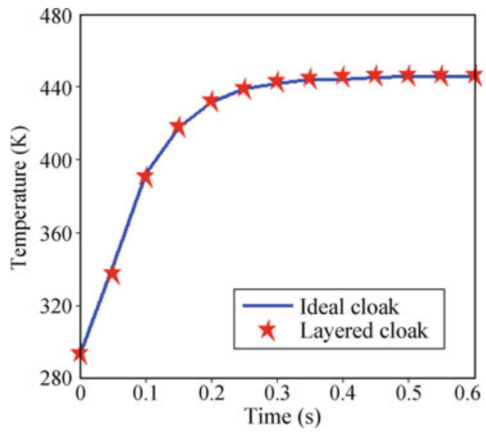

Fig. 7 Temperature changes as a function of time for the cloaking region of the 2D ideal and layered transient thermal cloak.

thermal cloaking effect of 3D diamond-shaped transient cloaks.

Finally, we examined whether or not the proposed layered cloak, consisting of only four types of isotropic materials, may function efficiently. Figure 6 illustrates the time-dependent temperature distribution for the 2D layered transient thermal cloak. In the simulation, regions I and II in the different quadrants were divided into ten layers that were sufficiently large to maintain the cloak's performance. The solid lines and arrows in the figure correspond to the isothermal lines and the thermal flux, respectively. Comparing Fig. 6 with Figs. 3(a)–(c), it is clear that for this case of the 2D layered thermal cloak, the temperature distribution at different times is in a good agreement with that for the ideal case. In addition, the isothermal lines and the thermal flux detour the cloaking region while being unperturbed elsewhere. To quantitatively evaluate the performance of the layered transient thermal cloak, we simulated temperature changes as a function of time for the cloaking region of the 2D ideal and layered cloaks, and the results are shown in Fig. 7. It can be seen that, for both cloaks, the temperature inside the cloaking region increases quickly with time. After the thermal equilibrium is reached for $t > 0.25$ s, the temperature remains at 446.8 K. In this process, we note that, for the two types of cloaks, the temperature inside the cloaking region at different times is practically the same. Hence, based on the above observations we conclude that a layered transient thermal cloak consisting of only alternating isotropic materials is feasible.

4 Conclusion

Based on transformation thermodynamics, both 2D and 3D diamond-shaped transient thermal cloaks with non-singular homogeneous material parameters were designed by expanding a line segment into a region along the orthogonal direction. The general expressions for the material parameters were derived and the performance of the proposed cloaks was validated by performing numerical simulations. Furthermore, to eliminate anisotropic material properties, we also proposed a 2D layered version of the cloak consisting of only four types of isotropic materials. The results reveal that the layered cloak behaves nearly as perfectly as the ideal one. It is believed that the scheme presented here can be applied to design other thermal devices and also be extended to the steady state or other branches of physics, such as acoustics and plasmonics.

Acknowledgements This work was supported by the National Natural Science Foundation of China (Grant Nos. 61161007 and 61261002), the Specialized Research Fund for the Doctoral Program of Higher Education (Grant No. 20135301110003), the Key Program of Natural Science of Yunnan Province (Grant No. 2013FA006), and the Fostering Foundation for the Excellent Ph.D.

Dissertation of Yunnan University (Grant No. XT512004).

References

1. J. B. Pendry, D. Schurig, and D. R. Smith, Controlling electromagnetic fields, *Science* 312(5781), 1780 (2006)
2. U. Leonhardt, Optical conformal mapping, *Science* 312(5781), 1777 (2006)
3. H. Y. Chen, C. T. Chan, and P. Sheng, Transformation optics and metamaterials, *Nat. Mater.* 9(5), 387 (2010)
4. D. H. Werner and D. H. Kwon, Transformation Electromagnetics and Metamaterials, London: Springer-Verlag, 2015
5. W. Li, J. G. Guan, Z. G. Sun, W. Wang, and Q. J. Zhang, A near-perfect invisibility cloak constructed with homogeneous materials, *Opt. Express* 17(26), 23410 (2009)
6. D. Bao, E. Kallos, W. X. Tang, C. Argyropoulos, Y. Hao, and T. J. Cui, A broadband simplified free space cloak realized by nonmagnetic dielectric cylinders, *Front. Phys.* 5(3), 319 (2010)
7. M. R. Forouzeshfard and M. Hosseini Farzad, Twin invisibility cloak at a distance and its illusory properties, *Plasmonics* 10(1), 125 (2015)
8. M. M. Sadeghi, H. Nadgaran, and H. Y. Chen, Perfect field concentrator using zero index metamaterials and perfect electric conductors, *Front. Phys.* 9(1), 90 (2014)
9. J. Yi, S. N. Burokur, G.P. Piau, and A. de Lustrac, Coherent beam control with an all-dielectric transformation optics based lens, *Sci. Rep.* 6, 18819 (2016)
10. F. Sun and S. L. He, Overlapping illusions by transformation optics without any negative refraction material, *Sci. Rep.* 6, 19130 (2016)
11. H. Y. Chen and C. T. Chan, Acoustic cloaking and transformation acoustics, *J. Phys. D Appl. Phys.* 43(11), 113001 (2010)
12. M. Farhat, S. Guenneau, and S. Enoch, Ultrabroadband elastic cloaking in thin plates, *Phys. Rev. Lett.* 103(2), 024301 (2009)
13. G. R. Mohammadi, A. G. Moghaddam, and R. Mohammadkhani, Coordinate transformations and matter waves cloaking, *Phys. Lett. A* 380(9–10), 1093 (2016)
14. W. R. Zhu, I. D. Rukhlenko, and M. Premaratne, Linear transformation optics for plasmonics, *J. Opt. Soc. Am. B* 29(10), 2659 (2012)
15. L. W. Zeng and R. X. Song, Controlling chloride ions diffusion in concrete, *Sci. Rep.* 3, 3359 (2013)
16. U. Leonhardt, Applied physics: Cloaking of heat, *Nature* 498(7455), 440 (2013)
17. C. Z. Fan, Y. Gao, and J. P. Huang, Shaped graded materials with an apparent negative thermal conductivity, *Appl. Phys. Lett.* 92(25), 251907 (2008)
18. G. X. Yu, Y. F. Lin, G. Q. Zhang, Z. Yu, L. L. Yu, and J. Su, Design of square-shaped heat flux cloaks and concentrators using method of coordinate transformation, *Front. Phys.* 6(1), 70 (2011)
19. T. Z. Yang, L. J. Huang, F. Chen, and W. K. Xu, Heat flux and temperature field cloaks for arbitrarily shaped objects, *J. Phys. D Appl. Phys.* 46(30), 305102 (2013)
20. F. C. Mao, T. H. Li, M. Huang, J. J. Yang, and J. C. Chen, Research and design of thermal cloak in arbitary shape, *Acta Physica Sinica* 63(1), 014401 (2014) (in Chinese)
21. T. C. Han, T. Yuan, B. W. Li, and C. W. Qiu, Homogeneous thermal cloak with constant conductivity and tunable heat localization, *Sci. Rep.* 3, 1593 (2013)
22. S. Narayana and Y. Sato, Heat flux manipulation with engineered thermal materials, *Phys. Rev. Lett.* 108(21), 214303 (2012)
23. E. H. Ooi and V. Popov, Transformation thermodynamics for heat flux management based on segmented thermal cloaks, *Eur. Phys. J. Appl. Phys.* 63(1), 10903 (2013)
24. S. Guenneau, C. Amra, and D. Veynante, Transformation thermodynamics: Cloaking and concentrating heat flux, *Opt. Express* 20(7), 8207 (2012)
25. R. Schittny, M. Kadic, S. Guenneau, and M. Wegener, Experiments on transformation thermodynamics: Molding the flow of heat, *Phys. Rev. Lett.* 110(19), 195901 (2013)
26. T. C. Han, X. Bai, J. T. L. Thong, B. W. Li, and C. W. Qiu, Full control and manipulation of heat signatures: Cloaking, camouflage and thermal metamaterials, *Adv. Mater.* 26(11), 1731 (2014)
27. T. C. Han, X. Bai, D. L. Gao, J. T. L. Thong, B. W. Li, and C. W. Qiu, Experimental demonstration of a bilayer thermal cloak, *Phys. Rev. Lett.* 112(5), 054302 (2014)
28. H. Y. Xu, X. H. Shi, F. Gao, H. D. Sun, and B. L. Zhang, Ultrathin three-dimensional thermal cloak, *Phys. Rev. Lett.* 112(5), 054301 (2014)
29. Y. G. Ma, L. Lan, W. Jiang, F. Sun, and S. L. He, A transient thermal cloak experimentally realized through a rescaled diffusion equation with anisotropic thermal diffusivity, *NPG Asia Mater.* 5(11), e73 (2013)
30. X. He and L. Z. Wu, Design of two-dimensional open cloaks with finite material parameters for thermodynamics, *Appl. Phys. Lett.* 102(21), 211912 (2013)
31. Y. Gao and J. P. Huang, Unconventional thermal cloak hiding an object outside the cloak, *Europhys. Lett.* 104(4), 44001 (2013)
32. R. Hu, X. L. Wei, J. Y. Hu, and X. B. Luo, Local heating realization by reverse thermal cloak, *Sci. Rep.* 4, 3600 (2014)
33. D. M. Nguyen, H. Y. Xu, Y. M. Zhang, and B. L. Zhang, Active thermal cloak, *Appl. Phys. Lett.* 107(12), 121901 (2015)
34. S. Guenneau and C. Amra, Anisotropic conductivity rotates heat fluxes in transient regimes, *Opt. Express* 21(5), 6578 (2013)
35. T. C. Han, J. J. Zhao, T. Yuan, D. Y. Lei, B. W. Li, and C. W. Qiu, Theoretical realization of an ultra-efficient thermal-energy harvesting cell made of natural materials, *Energy Environ. Sci.* 6(12), 3537 (2013)
36. Y. C. Liu, F. Sun, and S. L. He, Novel thermal lens for remote heating/cooling designed with transformation optics, *Opt. Express* 24(6), 5683 (2016)